[Global Biogeochemical Cycles]

Supporting Information for

Bacterial community structure modulates soil phosphorus turnover at early stages of primary succession

Yuhan Wang [1], Haijian Bing [2 *], Daryl L. Moorhead [3], Enqing Hou [4], Yanhong Wu [2], Jipeng Wang [5], Chengjiao Duan [6], Qingliang Cui [6], Zhiqin Zhang [7], He Zhu [2], Tianyi Qiu [1, 7], Zhongmin Dai [8], Wenfeng Tan [9], Min Huang [1], Hans Lambers [10], Peter B. Reich [11, 12], Linchuan Fang [1, 6 *]

[1] Key Laboratory of Green Utilization of Critical Non-metallic Mineral Resources, Ministry of Education, Wuhan University of Technology, Wuhan 430070, China

[2] Institute of Mountain Hazards and Environment, Chinese Academy of Sciences, Chengdu 610299, China

[3] Department of Environmental Sciences, University of Toledo, Toledo, OH 43606, USA

[4] Key Laboratory of Vegetation Restoration and Management of Degraded Ecosystems, South China Botanical Garden, Chinese Academy of Sciences, Guangzhou 510000, China

[5] CAS Key Laboratory of Mountain Ecological Restoration and Bioresource Utilization and Ecological Restoration and Biodiversity Conservation Key Laboratory of Sichuan Province, Chengdu Institute of Biology, Chinese Academy of Sciences, Chengdu 610041, China

[6] State Key Laboratory of Soil Erosion and Dryland Farming on the Loess Plateau, Institute of Soil and Water Conservation CAS and MWR, Yangling 712100, China

[7] College of Natural Resources and Environment, Northwest A&F University, Yangling 712100, China

[8] Institute of Soil and Water Resources and Environmental Science, College of Environmental and Resource Sciences, Zhejiang University, Hangzhou 310058, China

[9] State Environmental Protection Key Laboratory of Soil Health and Green Remediation, College of Resources and Environment, Huazhong Agricultural University, Wuhan 430070, China

[10] School of Biological Sciences, University of Western Australia, Perth, WA 6009, Australia

[11] Institute for Global Change Biology and School for Environment and Sustainability, University of Michigan, Ann Arbor, MI 48109, USA

[12] Department of Forest Resources, University of Minnesota, St. Paul, MN 55455, USA

* **Corresponding authors:**

Haijian Bing, E-mail address: hjbing@imde.ac.cn

Linchuan Fang, E-mail address: flinc629@hotmail.com

Contents of this file:

1. Supplementary methods

2. Supplementary tables (Table S1)

3. Supplementary figures (Figure S1-Figure S6)

1. Supplementary methods

Samples with a primary band length within the normal range (400-450 bp) of the PCR products detected by 1% agarose gel electrophoresis can be used for further experiments. GeneTools Analysis Software (Version4.03.05.0, SynGene) was used to compare PCR product concentrations and mix each PCR product according to the equal mass principle. The PCR mix was recovered using the E.Z.N.A.® Gel Extraction Kit (Omega, USA) and the target DNA fragments were recovered by elution in TE buffer following the NEBNext® Ultra™ DNA Library Prep Kit for Illumina® standard procedure for library building. Finally, the constructed amplicon libraries were sequenced by PE250 using the Illumina Hiseq2500 platform (Guangdong Magigene Biotechnology Co., Ltd. Guangzhou, China). The raw data were filtered and quality control required that reads containing N or mass below 20 and length below 100bp were filtered, and each pair of PE reads was spliced using FLASH (V1.2.11, https://ccb.jhu.edu/software/FLASH/) software to obtain the original splice sequence (Raw Tags), Mothur software (V1.35.1, http://www.mothur.org) then was used to assign sequences to the samples, remove barcode and primers, and finally get the valid splice fragment (Clean Tags). The Clean Tags of all samples were clustered into OTUs (Operational Taxonomic Units) with 97% agreement using the "uparse" method of Usearch software (V10, http://www.drive5.com/usearch/). The representative sequences of each OTU after removal of chimeras and singletons were compared with Silva (https://www.arb-silva.de/) Database comparisons to obtain 16S species annotation information, including species classification annotation results at different levels.

Table S1 The encoded protein and the functional processes of the phosphorus cycle encoded by each gene

Gene	Encoded protein	Functional process	Forward sequence (5′ → 3′)	Reverse sequence (5′ → 3′)
phnK	Putative phosphonate transport system ATP-binding protein	Po mineralization	CATCGTCGGCGAATCCGG	TGCTGCATGCCGCCGGAAAA
phoD	Alkaline phosphatase D	Po mineralization	CAGTGGGACGACCACGAGGT	GAGGCCGATCGGCATGTCG
phoX	Alkaline phosphatase/Pho regulon	Po mineralization	GARGAGAACWTCCACGGYTA	GATCTCGATGATRTGRCCRAAG
bpp	β-propeller phytase	Po mineralization	GACGCAGCCGAYGAYCCNGCNITNTGG	CCRTCSGGGAAGTAGTTKCC
ppx	Exopolyphosphatase	polyP hydrolysis	TGCATCTGGCGGACGGCCT	AGATCCGCCGCCAATATCA
pqqC	Pyrroloquinoline-quinone synthase	P_i solubilization	AACCGCTTCTACTACCAG	GCGAACAGCTCGGTCAG
cphy	Pyrroloquinoline-quinone synthase	P_i solubilization	GTGGACCTRCGRMARGARWCICA	GTCCGACCATTGCCTGCYTCRCARTGRAMRTGIADCCA
ppk3	Polyphosphate kinase	polyP biosynthesis	GACCCGAABGTRCTBGCSAT	TTATAATTNCCSGTNCCNA

Note: P_O mineralization: organic P mineralization, polyP hydrolysis: polyphosphate hydrolysis, P_i solubilization: inorganic P solubilization, polyP biosynthesis: polyphosphate biosynthesis.

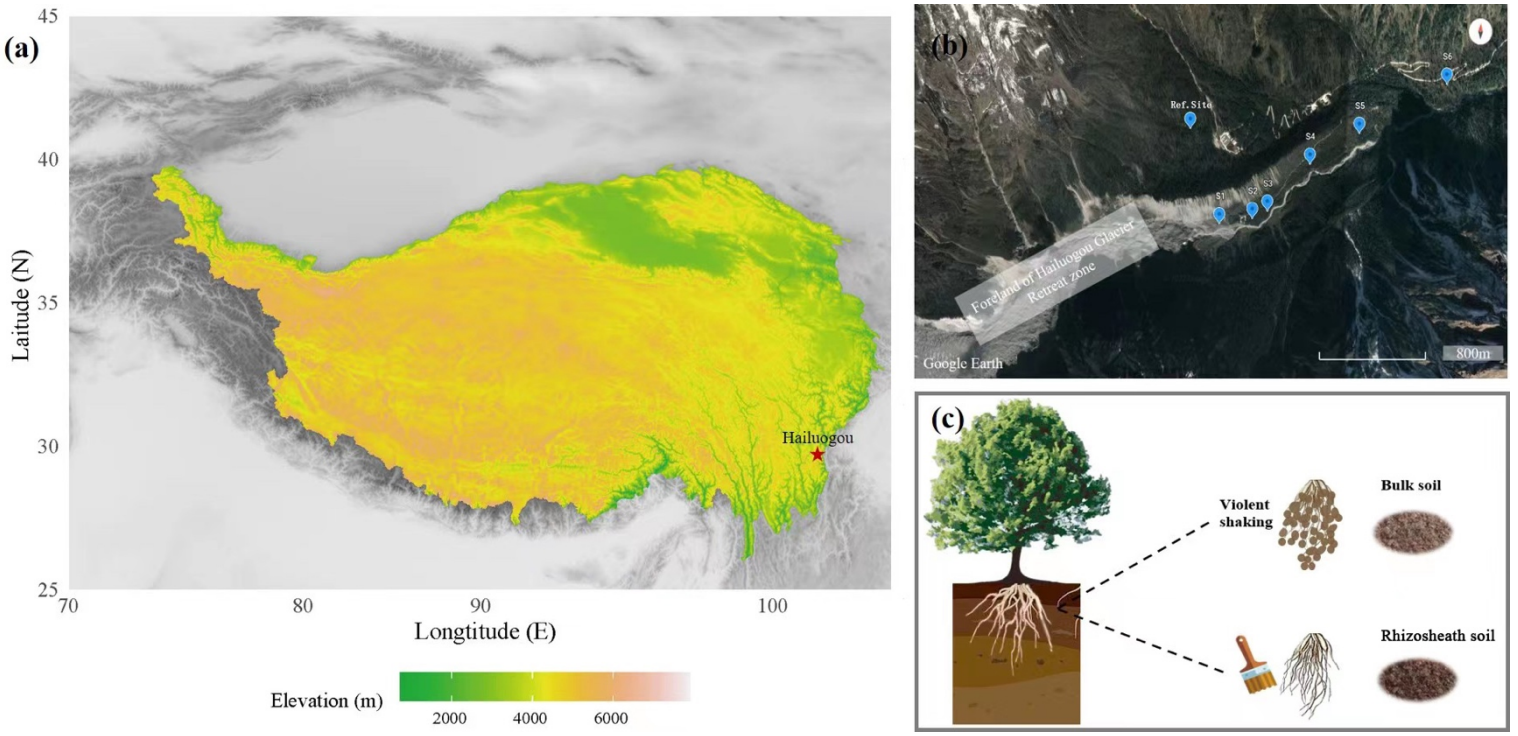


Figure S1. The location of Hailuogou glacial chronosequence, eastern Tibetan Plateau (a), and sampling sites along the Hailuogou glacial chronosequence (b). Collection of samples from the rhizosheath and bulk soil of dominant species (c).

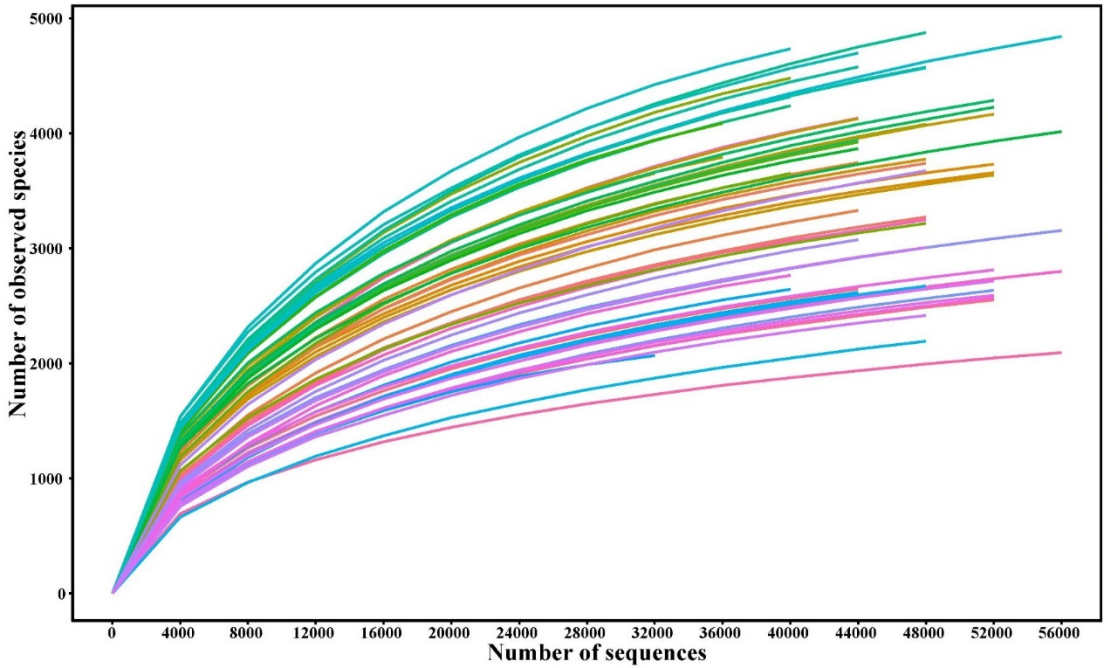


Figure S2. Rarefaction curves of the 16S rRNA gene sequencing. The 56 samples were represented by different colors. Rarefaction curves plateaued or began to plateau at a sequencing depth of the lowest sequencing number for 16S rRNA genes, indicating that sequencing had reached saturation.

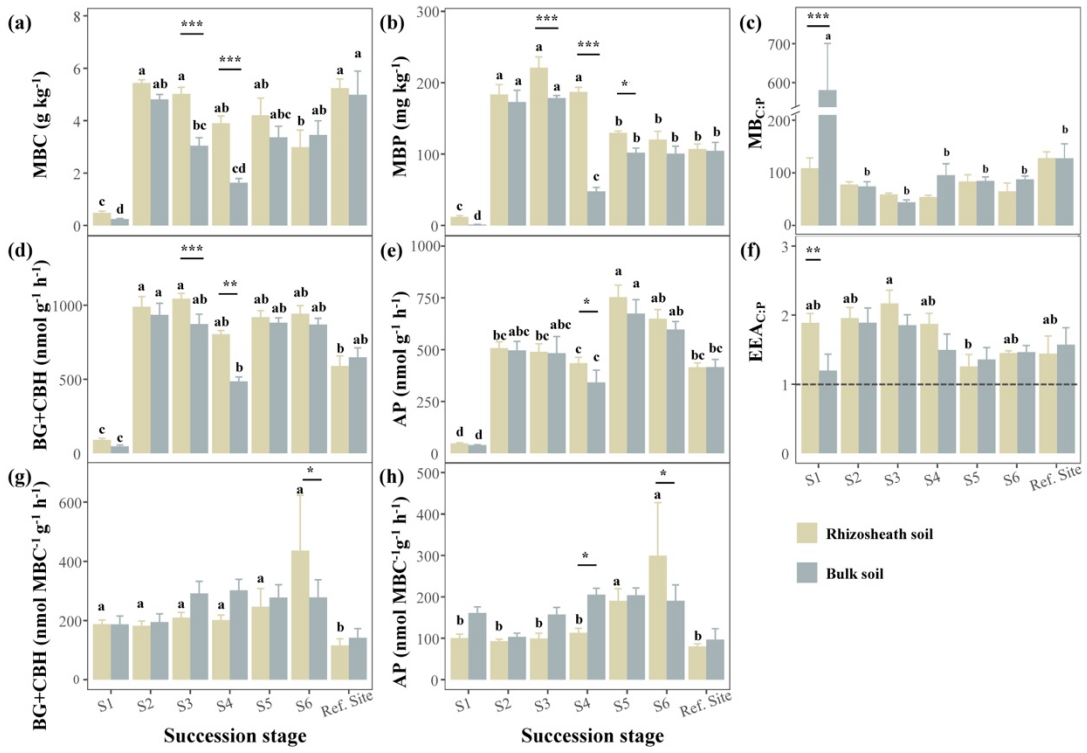


Figure S3. Microbial biomass, extracellular enzyme activities, and their ratios along the chronosequence and at the reference site. (a) microbial biomass carbon (MBC); (b) microbial biomass phosphorus (MBP); (c) the ratio of MBC to MBP (MBC:MBP); (d) the activity of C-acquiring enzymes (BG + CBH); (e) the activity of phosphorus (P)-acquiring enzymes (AP); (f) the ratio of carbon (C)-acquiring enzymes (BG + CBH) to P-acquiring enzyme (AP) ($EEA_{C:P}$), the black dashed line represents the activities of C versus P acquiring enzyme are equivalent. Each value represents the mean ± standard error (n = 4). Differences of means were tested using a mixed linear model. Different lowercase letters within a column type indicate significant differences among the stages in the bulk or rhizosheath soils ($P < 0.05$). The asterisks indicate significant differences between the bulk and rhizosheath soil at each stage. *, $P < 0.05$, **, $P < 0.01$, ***, $P < 0.001$.

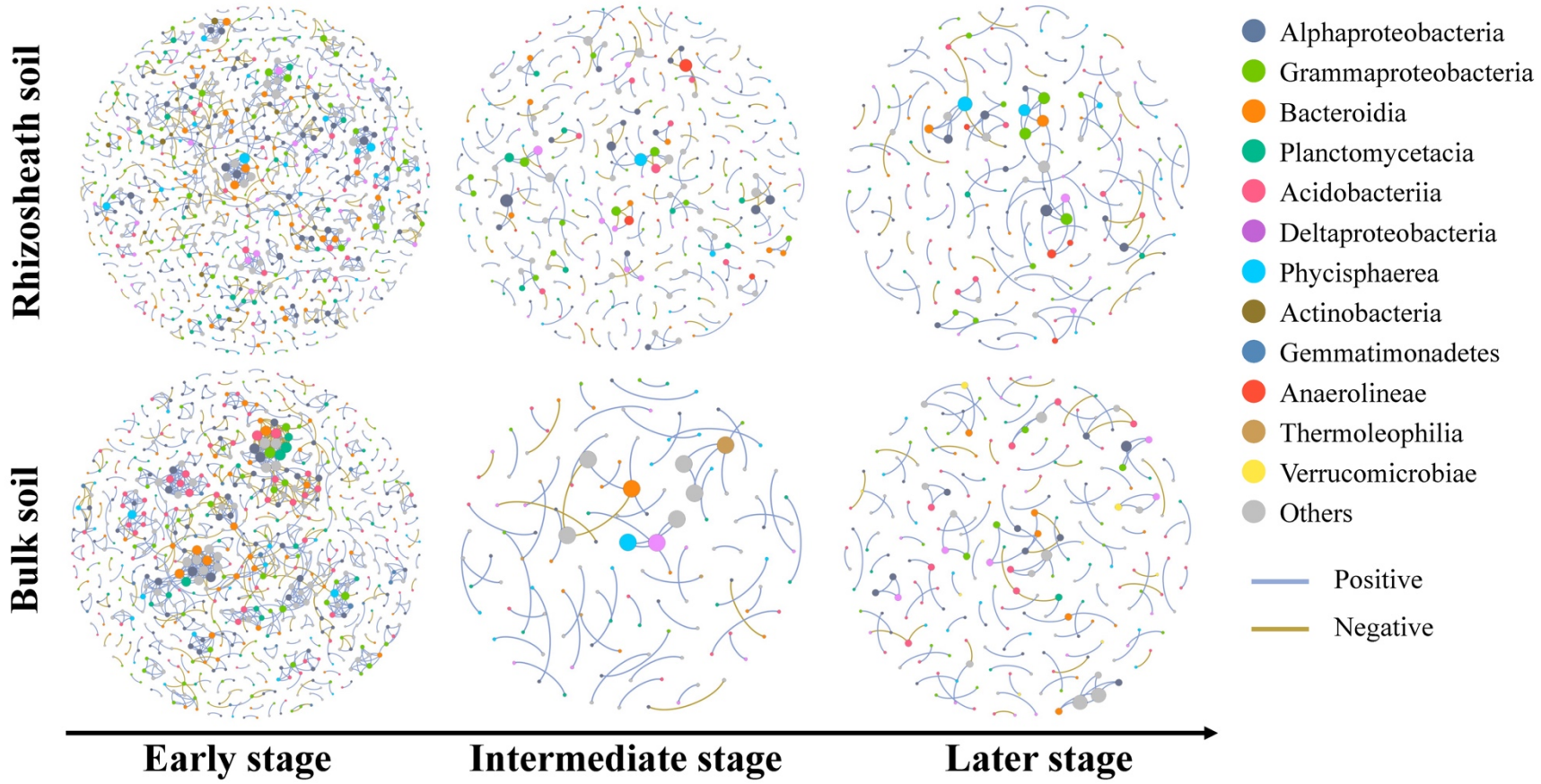


Figure S4. Co-occurrence patterns of bacterial community in the rhizosheath and bulk soils at early, intermediate, and later stages. Each node represents a bacterial taxon at the class level, and the size of each node is proportional to its number of links. Links of two nodes represent strong ($R > 0.8$) and significant ($P < 0.01$) correlations between bacterial taxa, the blue line represents a positive correlation, and the brown line represents a negative correlation.

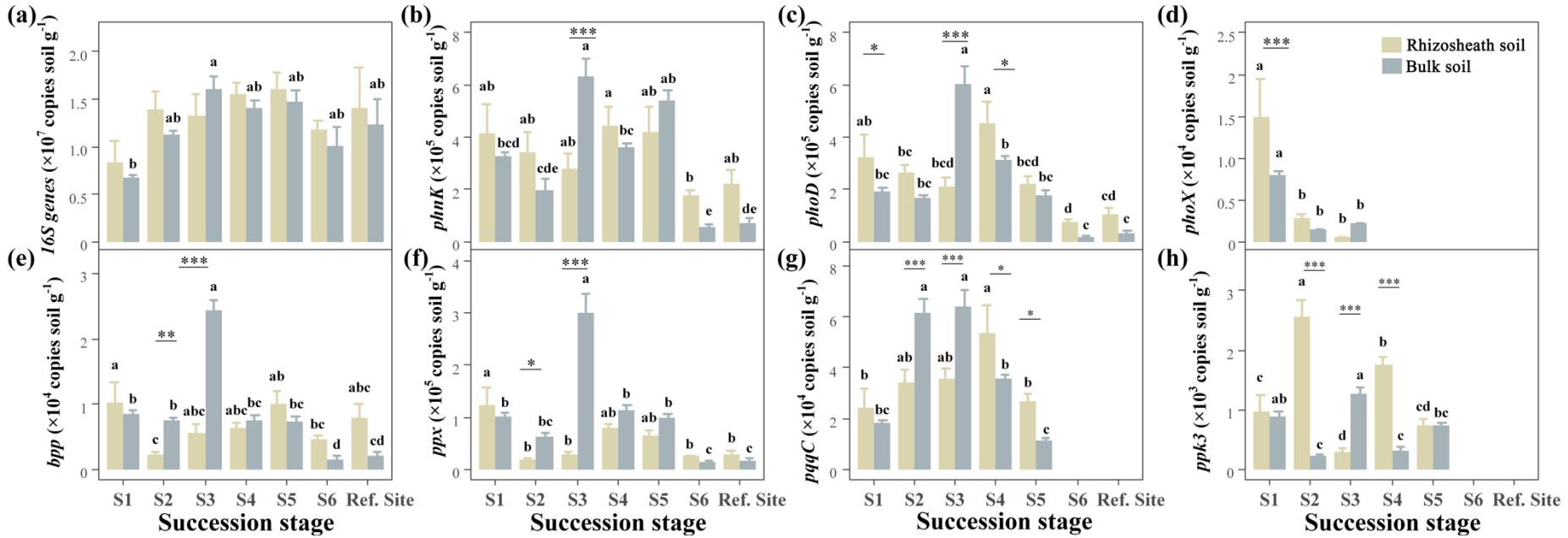
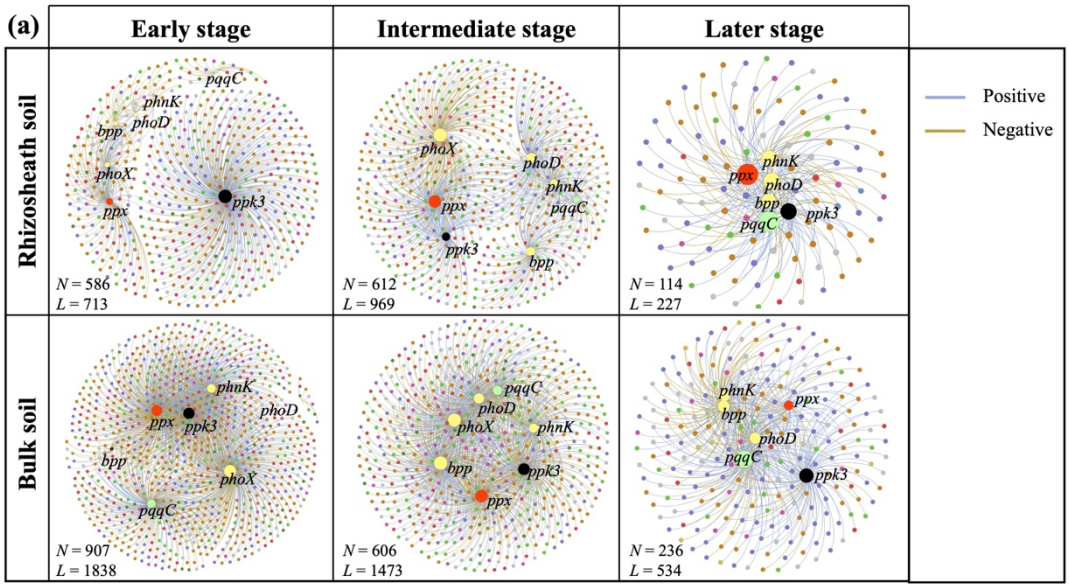


Figure S5. Absolute abundances of 16S and phosphorus (P)-cycling genes along the chronosequence and at the reference site. Each value represents the mean ± standard error (n = 4). Differences between means were tested with a mixed linear model. Different lowercase letters within a column indicate significant differences amongst succession stages in the bulk or rhizosheath soils ($P < 0.05$). The asterisks indicate significant differences between the bulk and rhizosheath soils at a stage. The CT values of *cphy* in all samples were greater than 31, no amplification was considered, so the abundance of *cphy* in the samples was 0, and is not shown in the figure. *, $P < 0.05$, **, $P < 0.01$, ***, $P < 0.001$.



(b)

	phnK		*phoD*		*phoX*		*bpp*		*ppx*		*pqqC*		*ppk3*		
	RS	BS	RS	BS	RS	BS	RS	BS	RS	BS	RS	BS	RS	BS	
Early stage	8	99	12	2	30	185	16	8	54	140	11	117	155	161	Proteobacteria
Intermediate stage	34	54	56	50	77	73	31	84	72	79	23	50	38	73	
Later stage	13	15	11	18	/	/	11	17	16	13	16	33	14	25	
Early stage	2	43	1	1	10	68	3	5	21	64	0	45	56	70	Acidobacteria
Intermediate stage	11	16	17	11	23	25	9	25	21	19	6	15	11	28	
Later stage	10	19	5	25	/	/	9	27	17	20	8	55	7	44	
Early stage	2	36	3	1	6	40	6	4	8	41	4	27	43	40	Planctomycetes
Intermediate stage	11	35	13	33	35	42	23	39	30	41	8	28	22	41	
Later stage	2	6	6	10	/	/	3	7	5	5	5	11	3	13	
Early stage	0	38	3	1	9	45	8	3	19	49	5	26	48	47	Bacteroidetes
Intermediate stage	7	7	14	13	15	14	16	19	17	11	3	5	7	8	
Later stage	1	4	1	2	/	/	1	5	1	3	2	5	3	6	
Early stage	3	24	3	1	11	32	7	0	11	31	1	13	26	34	Actinobacteria
Intermediate stage	5	9	6	29	10	36	7	45	10	36	3	19	3	19	
Later stage	2	7	3	4	/	/	1	7	1	4	2	7	1	4	
Early stage	1	16	1	2	2	31	2	1	4	21	1	18	15	27	Chloroflexi
Intermediate stage	9	8	12	6	18	16	6	12	13	10	3	9	7	13	
Later stage	0	1	0	1	/	/	0	1	1	0	0	4	0	2	
Early stage	0	1	0	0	0	6	0	0	1	3	0	4	2	3	Armatimonadetes
Intermediate stage	0	1	0	3	0	2	1	3	0	0	0	0	1	1	
Later stage	1	3	1	4	/	/	1	3	2	4	1	2	1	4	

Figure S6. Network visualization of bacterial taxa-gene co-occurrence patterns in the rhizosheath and bulk soil at early, intermediate, and later stages. (a) Taxa-gene co-occurrence networks at the phylum level. N: nodes, L: links. Each node represents a bacterial taxon or a phosphorus (P)-cycling gene, and the size of each node is proportional to its number of links. Links of two nodes represent strong ($R > 0.8$) and significant ($P < 0.05$) correlations between bacterial taxa and P-cycling genes; the blue line represents a positive correlation, and the brown line represents a negative correlation. (b) Number of links for taxa and genes in each co-occurrence network. RS: rhizosheath soil; BS: bulk soil.